Int. J. Heat Mass Transfer. Vol. 9, pp. 803–817. Pergamon Press 1966. Printed in Great Britain

FORCED CONVECTIVE HEAT TRANSFER BETWEEN HORIZONTAL FLAT PLATES

YASUO MORI and YUTAKA UCHIDA
Department of Mechanical Engineering, Tokyo Institute of Technology

(*Received* 14 *January* 1966)

Abstract—In fully developed flows and temperature fields between two horizontal flat plates (when the lower plate is heated and the upper one is cooled), the phenomenon might be considered to be two-dimensional. However, when the temperature difference between these flat plates is increased above a critical value, vortex rolls with their axes parallel to the flow direction are observed to appear between the flat plates. Consequently, the flow and temperature fields are completely affected by these vortex rolls and have a three-dimensional character. The momentum and energy equations for such fields are non-linear. These equations are solved approximately on the basis of energy and entropy production balance of vortex rolls. In order to ascertain theoretical results, the velocity and temperature distributions of the three-dimensional flow are measured. It is found that theoretical results are in good agreement with experimental results.

NOMENCLATURE

x, co-ordinate parallel to the main flow direction (see Fig. 1);
y, co-ordinate normal to the horizontal flat plates (see Fig. 1);
z, co-ordinate parallel to the horizontal flat plates and normal to the main flow direction (see Fig. 1);
u, velocity component in the x-direction;
v, velocity component in the y-direction;
w, velocity component in the z-direction;
U_0, maximum value of the fully developed velocity profile with no vortex rolls;
P, pressure;
ρ, density;
ν, kinematic viscosity;
C_p, specific heat of fluid at constant pressure;
k, heat conductivity;
T, temperature;
T_w, surface temperature of the heated horizontal flat plate (constant);
T_u, surface temperature of the cooled horizontal flat plate (constant);
ΔT, temperature difference, $T_w - T_u$;
q, heat transfer from the lower to the upper flat plate;
β, coefficient of thermal expansion;
g, acceleration due to gravity;
d, thickness of the passage;
λ, pitch of vortex rolls;
Re, Reynolds number, $U_0 d/\nu$;
Pr, Prandtl number, $\rho\nu C_p/k$;
Gr, Grashof number, $g\beta\Delta T d^3/\nu^2$;
Ra, Rayleigh number, $Pr \cdot Gr$;
Nu, Nusselt number, $qd/k\Delta T$;

1. INTRODUCTION

CONSIDER a flow between two horizontal flat plates, where the lower plate is heated isothermally and the upper one is cooled isothermally. When the temperature difference between these flat plates is small and the flow and temperature fields are fully developed in the flow direction, the profiles of velocity and temperature distributions are respectively parabolic and linear. In the following, such a state of flow is called the main stream.

When the temperature difference between the horizontal flat plates is increased above a critical value, longitudinal vortex rolls appear in the passage. The flow pattern is completely affected by these vortices. These vortices are generated by buoyancy. The fluid motion in a closed horizontal fluid layer which is heated

from below was first analysed by Lord Rayleigh and has since been studied by many researchers. Recently, analytical and experimental work on this problem has been done by Malkus [1, 2]. He intended to explain the nature of turbulence using the mechanism of convective cells caused by buoyancy. However, no quantitative measurement for such a convective cell has been made, because the cellular motion is too unstable to be measured. The low velocity of the cellular motion has also made it difficult to measure the velocity distribution.

In this study, the obstacle is removed by the existence of the main stream, and quantitative measurements are made. Experimental results are compared with analytical results and a fairly good agreement is obtained.

Usually, a flow between two horizontal flat plates is treated as a two-dimensional phenomenon and the three-dimensional character caused by vortex rolls is not considered. The flow can be treated as a two-dimensional phenomenon only when the temperature difference between the flat plates is small. In the case of a finite temperature difference, which is important practically, vortex rolls appear in the passage and the heat transfer from the lower to the upper plate increases. If the temperature difference is increased further, the vortex rolls split and the size of each roll decreases. Eventually, the regularity of the fluid motion disappears and turbulence occurs.

Consider the mechanism of such a vortex roll. If we observe one vortex roll, it is known that it absorbs (a) energy introduced into the vortex roll by buoyancy, (b) energy introduced into the vortex roll from the main stream by the Reynolds stress, and (c) energy introduced into the vortex roll from larger-scale vortex rolls by the interaction of vortex rolls. These energies are balanced by (a) energy transferred from this roll to smaller-scale vortex rolls and (b) energy dissipated by viscosity. There seems to exist a resemblance between this mechanism and the turbulent flow mechanism. Therefore, the object of this report is not only to consider the effect of buoyancy on the forced convective heat transfer, but also to clarify the basic concept of turbulence by means of the analogy which exists between a discrete vortex roll system and turbulence.

2. ANALYSIS

2.1 *Basic equations*

The co-ordinate system is indicated in Fig. 1. Dividing velocity, length, temperature and pressure by U_0, d, ΔT, and $\rho_s U_0^2$, respectively, we obtain non-dimensional expressions, where the suffix s means the standard state. Then,

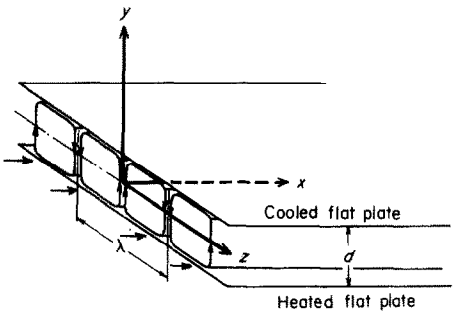

FIG. 1. The co-ordinate system.

$$(u,v,w) = U_0(u^*,v^*,w^*),$$
$$(x,y,z) = d(x^*,y^*,z^*), \qquad T = \Delta T \,.\, T^*,$$
$$T_w = \Delta T \,.\, T_w^*, \qquad T_u = \Delta T \,.\, T_u^*,$$
$$P = \rho_s U_0^2 \,.\, P^*.$$

Having made this change, all stars will now be dropped. In the remainder of this report all unstarred quantities are non-dimensional unless it is otherwise stated.

Let us consider a steady fully developed flow in the x-direction and assume that fluid properties except ρ are always independent of temperature. Moreover, we assume that the density variation due to the temperature difference appears only in one term where ρ is multiplied by g. This variation is indicated approximately as

$$\rho g = \rho_s\{1 - \beta\,\Delta T(T - T_s)\}\, g.$$

Velocity, pressure and temperature are written

as follows:

$$\left.\begin{aligned} u &= \bar{u}(y) + u'(y,z) \\ v &= v'(y,z) \\ w &= w'(y,z) \\ P &= \bar{P}(x,y) + P'(y,z) \\ T &= \bar{T}(y) + T'(y,z) \end{aligned}\right\} \quad (1)$$

In contrast to the time mean in a turbulent flow, the bars in equation (1) indicate a mean value taken over the z-direction. Terms with bars and primes indicate mean values and fluctuation components, respectively. All fluctuation components have a periodicity in the z-direction and their mean values over one pitch reduce to zero. That is,

$$\overline{u'} = \overline{v'} = \overline{w'} = \overline{P'} = \overline{T'} = 0.$$

Substituting equation (1) into the Navier–Stokes equation and the energy equation, neglecting pressure and dissipation terms and making use of the characteristics of fluctuation components, we obtain equations for the mean flow and fluctuation components. In the above process, we put the pressure gradient $\partial P/\partial x$ equal to the well-known value, $-8/Re$, which corresponds to a two-dimensional channel flow.

The equations for the fluctuation components are

$$\frac{\partial v'}{\partial y} + \frac{\partial w'}{\partial z} = 0 \quad (2)$$

$$v'\frac{\partial \bar{u}}{\partial y} + v'\frac{\partial u'}{\partial y} + w'\frac{\partial u'}{\partial z} - \frac{\partial \overline{u'v'}}{\partial y} = \frac{1}{Re}\left(\frac{\partial^2 u'}{\partial y^2} + \frac{\partial^2 u'}{\partial z^2}\right) \quad (3)$$

$$v'\frac{\partial v'}{\partial y} + w'\frac{\partial v'}{\partial z} - \frac{\partial \overline{v'^2}}{\partial y} = -\frac{\partial P'}{\partial y} + \frac{1}{Re}\left(\frac{\partial^2 v'}{\partial y^2} + \frac{\partial^2 v'}{\partial z^2}\right) + \frac{Gr}{Re^2}T' \quad (4)$$

$$v'\frac{\partial w'}{\partial y} + w'\frac{\partial w'}{\partial z} = -\frac{\partial P'}{\partial z} + \frac{1}{Re}\left(\frac{\partial^2 w'}{\partial y^2} + \frac{\partial^2 w'}{\partial z^2}\right) \quad (5)$$

$$v'\frac{\partial \bar{T}}{\partial y} + v'\frac{\partial T'}{\partial y} + w'\frac{\partial T'}{\partial z} - \frac{\partial \overline{v'T'}}{\partial y} = \frac{1}{PrRe}\left(\frac{\partial^2 T'}{\partial y^2} + \frac{\partial^2 T'}{\partial z^2}\right) \quad (6)$$

The equations for the mean stream are

$$\frac{\partial \overline{u'v'}}{\partial y} = \frac{8}{Re} + \frac{1}{Re}\frac{\partial^2 \bar{u}}{\partial y^2} \quad (7)$$

$$\frac{\partial \overline{v'T'}}{\partial y} = \frac{1}{PrRe}\frac{\partial^2 \bar{T}}{\partial y^2} \quad (8)$$

Equations (2) to (8) are non-linear and cannot be solved exactly. Therefore, we solve these equations approximately by the following method. In the first place, these equations are linearized and the form of each fluctuation component is solved. Then using the energy and entropy production balance equations for fluctuation components which include the non-linear effect, the amplitude for each fluctuation component is determined. Distributions of fluctuation components and the mean flow are described by the use of these forms and amplitudes. This method is a modification of the technique that was used by Stuart [3] to solve the flow between rotating concentric cylinders with Taylor vortex rolls.

2.2 *Linearized theory*

Assume fluctuation components as follows:

$$\left.\begin{aligned} u' &= u'_1(y)\cos\alpha_1 z + u'_2(y)\cos\alpha_2 z \\ v' &= v'_1(y)\cos\alpha_1 z + v'_2(y)\cos\alpha_2 z \\ w' &= w'_1(y)\sin\alpha_1 z + w'_2(y)\sin\alpha_2 z \\ P' &= P'_1(y)\cos\alpha_1 z + P'_2(y)\cos\alpha_2 z \\ T' &= T'_1(y)\cos\alpha_1 z + T'_2(y)\cos\alpha_2 z \end{aligned}\right\} \quad (9)$$

where

$$\alpha = \frac{2\pi}{\lambda}d.$$

In equation (9) suffixes 1 and 2 indicate the first and second type vortex rolls, respectively. The first type vortex rolls correspond to those which appear at first in the passage when the

temperature difference between the flat plates is gradually increased. If the temperature difference is increased further, the second type vortex rolls appear in the passage. Due to the larger temperature difference, higher-order vortex rolls appear, but, to avoid the complexity, only the region with the first and the second type vortex rolls is considered. The first and the second type vortex rolls are schematically shown in Fig. 2.

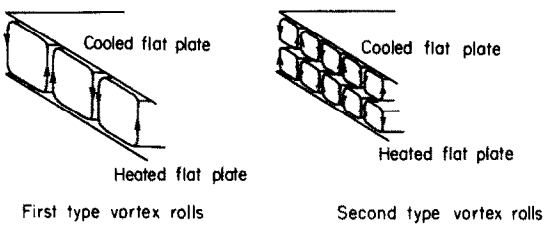

FIG. 2. Patterns of vortex rolls.

As this is a linearized theory, the mean flow is not affected by fluctuations and is expressed as follows:

$$\left.\begin{aligned} \bar{u} &= 1 - 4y^2 \\ \bar{T} &= -(y + \tfrac{1}{2}) + T_w \\ \frac{\partial \bar{P}}{\partial x} &= -\frac{8}{Re} \end{aligned}\right\} \quad (10)$$

Substituting equations (9) and (10) into equations (2) to (6) and linearizing the fluctuation components, we obtain equations for the first and the second type vortex roll components.

Equations for the first type vortex roll components are

$$w_1' = -\frac{1}{\alpha_1}\frac{\mathrm{d}v_1'}{\mathrm{d}y} \quad (11)$$

$$\left(\frac{\mathrm{d}^2}{\mathrm{d}y^2} - \alpha_1^2\right) u_1' = -8Re\, v_1' y \quad (12)$$

$$\left(\frac{\mathrm{d}^2}{\mathrm{d}y^2} - \alpha_1^2\right)^2 v_1' = \frac{\alpha_1^2 Gr}{Re} T_1' \quad (13)$$

$$\left(\frac{\mathrm{d}^2}{\mathrm{d}y^2} - \alpha_1^2\right) T_1' = -PrRe\, v_1'. \quad (14)$$

Equations for the second type vortex roll components are

$$w_2' = -\frac{1}{\alpha_2}\frac{\mathrm{d}v_2'}{\mathrm{d}y} \quad (15)$$

$$\left(\frac{\mathrm{d}^2}{\mathrm{d}y^2} - \alpha_2^2\right) u_2' = -8Re\, v_2' y \quad (16)$$

$$\left(\frac{\mathrm{d}^2}{\mathrm{d}y^2} - \alpha_2^2\right)^2 v_2' = \frac{\alpha_2^2 Gr}{Re} T_2' \quad (17)$$

$$\left(\frac{\mathrm{d}^2}{\mathrm{d}y^2} - \alpha_2^2\right) T_2' = -PrRe\, v_2'. \quad (18)$$

The boundary conditions for rigid conducting boundaries are written as follows:

$$v_1' = \frac{\mathrm{d}v_1'}{\mathrm{d}y} = \left(\frac{\mathrm{d}^2}{\mathrm{d}y^2} - \alpha_1^2\right)^2 v_1' = 0 \quad \text{at} \quad y = \pm\tfrac{1}{2} \quad (19)$$

$$v_2' = \frac{\mathrm{d}v_2'}{\mathrm{d}y} = \left(\frac{\mathrm{d}^2}{\mathrm{d}y^2} - \alpha_2^2\right)^2 v_2' = 0 \quad \text{at} \quad y = \pm\tfrac{1}{2}. \quad (20)$$

As equations (13), (14), (17) and (18) are not affected by $\bar{u}$, the eigenvalue problem considering the appearance of vortex rolls is not affected by $\bar{u}$ so long as the flow is fully developed in the x-direction.

From equations (13) and (14), we get

$$\left(\frac{\mathrm{d}^2}{\mathrm{d}y^2} - \alpha_1^2\right)^3 v_1' = -\alpha_1^2 Ra\, v_1' \quad (21)$$

From equations (17) and (18),

$$\left(\frac{\mathrm{d}^2}{\mathrm{d}y^2} - \alpha_2^2\right)^3 v_2' = -\alpha_2^2 Ra\, v_2'. \quad (22)$$

Equations (21) and (22) with the boundary conditions (19) and (20) form an eigenvalue problem which relates the Rayleigh number to the wave number α. This problem was solved by Pellew and Southwell [4] and the result is shown in Fig. 3. In Fig. 3, $(Ra)_1$ and $(Ra)_2$ mean the critical Rayleigh numbers for the first and the second type vortex rolls, respectively. As is shown in Fig. 3, the first type vortex rolls

with the wave number 3·13 appear at the lowest Rayleigh number 1708. Therefore, we put $\alpha_1 = 3{\cdot}13$. The wave number for the lowest $(Ra)_2$ is 5·36, but we assume here that α_2 is equal to $2\alpha_1$, and put $\alpha_2 = 6{\cdot}26$. The reason for this assumption is explained in the following section.

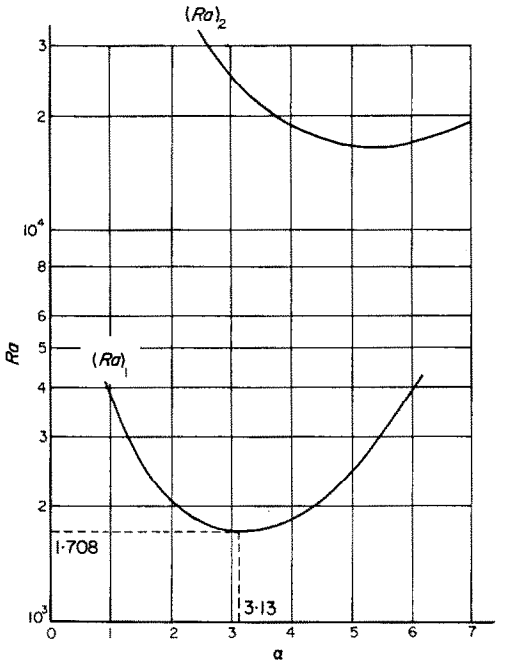

FIG. 3. Relation between the critical Rayleigh number and the wave number.

Putting $\alpha_1 = 3{\cdot}13$ and $\alpha_2 = 6{\cdot}26$, we can solve equations (11) to (18) and get

$$u_1' = -\frac{8A}{3{\cdot}13} Re \{-0{\cdot}121\, y \cos 4y + 0{\cdot}0376 \times \sin 4y - 0{\cdot}0165\, y \cos 2{\cdot}16\, y \cosh 5{\cdot}04\, y - 0{\cdot}00110\, y \sin 2{\cdot}16\, y \sinh 5{\cdot}04\, y + 0{\cdot}00517 \times \sin 2{\cdot}16\, y \cosh 5{\cdot}04\, y + 0{\cdot}00539 \times \cos 2{\cdot}16\, y \sinh 5{\cdot}04\, y - 0{\cdot}0334 \sinh 3{\cdot}13\, y\} = A f_1(y) \quad (23)$$

$$v_1' = A \{\cos 4y + 0{\cdot}111 \sin 2{\cdot}16\, y \sinh 5{\cdot}04\, y - 0{\cdot}0655 \cos 2{\cdot}16\, y \cosh 5{\cdot}04\, y\} = A g_1(y) \quad (24)$$

$$w_1' = A \{1{\cdot}28 \sin 4y + 0{\cdot}0284 \cos 2{\cdot}16\, y \times \sinh 5{\cdot}04\, y - 0{\cdot}224 \sin 2{\cdot}16\, y \cosh 5{\cdot}04\, y\} = A h_1(y) \quad (25)$$

$$T_1' = \frac{A}{3{\cdot}13} Pr\, Re \{0{\cdot}122 \cos 4y + 0{\cdot}0197 \times \cos 2{\cdot}16\, y \cosh 5{\cdot}04\, y + 0{\cdot}00116 \sin 2{\cdot}16\, y \times \sinh 5{\cdot}04\, y - 0{\cdot}00543 \cosh 3{\cdot}13\, y\} = A i_1(y) \quad (26)$$

$$u_2' = -\frac{4B}{3{\cdot}13} Re \{0{\cdot}0698\, y \sin 7{\cdot}11\, y + 0{\cdot}0111 \times \cos 7{\cdot}11\, y + 0{\cdot}000820\, y \sin 3{\cdot}91\, y \times \cosh 9{\cdot}59\, y + 0{\cdot}000561\, y \cos 3{\cdot}91\, y \times \sinh 9{\cdot}59\, y + 0{\cdot}0000295 \cos 3{\cdot}91\, y \times \cosh 9{\cdot}59\, y - 0{\cdot}000244 \sin 3{\cdot}91\, y \times \sinh 9{\cdot}59\, y + 0{\cdot}00190 \cosh 6{\cdot}26\, y\} = B f_2(y) \quad (27)$$

$$v_2' = -B \{\sin 7{\cdot}11\, y - 0{\cdot}0132 \cos 3{\cdot}91\, y \times \sinh 9{\cdot}59\, y + 0{\cdot}00181 \sin 3{\cdot}91\, y \sinh 9{\cdot}59\, y\} = B g_2(y) \quad (28)$$

$$w_2' = -B \{-1{\cdot}136 \cos 7{\cdot}11\, y + 0{\cdot}0190 \times \cos 3{\cdot}91\, y \cosh 9{\cdot}59\, y - 0{\cdot}0110 \sin 3{\cdot}91\, y \times \sinh 9{\cdot}59\, y\} = B h_2(y) \quad (29)$$

$$T_2' = -\frac{B}{6{\cdot}26} Pr\, Re \{0{\cdot}0698 \sin 7{\cdot}11\, y + 0{\cdot}000820 \sin 3{\cdot}91\, y \cosh 9{\cdot}59\, y + 0{\cdot}000561 \times \cos 3{\cdot}91\, y \sinh 9{\cdot}59\, y - 0{\cdot}000458 \times \sinh 6{\cdot}26\, y\} = B i_2(y). \quad (30)$$

A and B in the above equations are arbitrary constants.

Equations (23) to (30) give the forms of fluctuation components. Their amplitudes are determined in the next section.

2.3 *Energy integral*

The amplitudes of fluctuation components cannot be determined by linearized theory. To determine the amplitudes, the basic equations (2) to (8) which contain non-linear terms must be used. Using the relations obtained by

linearized theory, we put fluctuation components as follows:

$$\left.\begin{aligned} u' &= a f_1(y) \cos \alpha_1 z + d f_2(y) \cos 2\alpha_1 z \\ v' &= b g_1(y) \cos \alpha_1 z + e g_2(y) \cos 2\alpha_1 z \\ w' &= b h_1(y) \sin \alpha_1 z + e h_2(y) \sin 2\alpha_1 z \\ T' &= c i_1(y) \cos \alpha_1 z + f i_2(y) \cos 2\alpha_1 z \end{aligned}\right\} \quad (31)$$

In equation (31) a, b, c, d, e, f are the unknown amplitudes of each fluctuation component. By the assumption in the former section, α_1 is equal to 3·13.

It is clear from equations (4) and (5) that v' and w' are not affected by u'. Therefore, it is reasonable to distinguish between the amplitude of the fluctuation velocity component in the x-direction and those in the y- and z-directions. Then, the amplitude of the fluctuation velocity component in the x-direction must satisfy an x-directional energy balance equation.

Equation (31) is substituted into equation (3) and then each term is multiplied by $a f_1(y) \cos \alpha_1 z$ (x-directional velocity component of the first type vortex roll). Taking the average value of the above equation in the y–z plane, we get the following equation, equation (32). Notice must be taken of the fact that $\bar{u}$ and $\bar{T}$ satisfy equations (7) and (8).

$$\begin{aligned} &- \int_{-\frac{1}{2}}^{\frac{1}{2}} a b f_1(y) g_1(y) \left\{ -8y + \frac{Re}{2} [a b f_1(y) \right. \\ &\left. \times g_1(y) + d e f_2(y) g_2(y)] \right\} dy \\ &- \tfrac{1}{2} \int_{-\frac{1}{2}}^{\frac{1}{2}} \left\{ a f_1(y) \left[b d \frac{df_2(y)}{dy} g_1(y) \right.\right. \\ &\left. + a e \frac{df_1(y)}{dy} g_2(y) \right] - \alpha_1 [a f_1(y) \langle 2 b d f_2(y) \\ &\left. \times h_1(y) + a e f_1(y) h_2(y) \rangle] \right\} dy \\ &- \int_{-\frac{1}{2}}^{\frac{1}{2}} a^2 8 y f_1(y) g_1(y) dy = 0. \end{aligned} \quad (32)$$

Equation (32) indicates the x-directional energy balance equation for the first type vortex roll. The first term on the left-hand side of equation (32) represents the energy introduced into the first type vortex roll from the mean flow by means of the stress which might be called the Reynolds stress, although the mean value is taken over the z-direction, the second term the energy given by the first type vortex roll to the second type vortex roll by means of the interaction between these vortex rolls. The third term represents the energy dissipated by viscosity. Equation (32) shows that the first type vortex roll exists by such an x-directional energy balance mechanism.

Through the same calculation, the x-directional energy balance equation for all of the vortex rolls becomes as follows:

$$\begin{aligned} &- \int_{-\frac{1}{2}}^{\frac{1}{2}} [a b f_1(y) g_1(y) + d e f_2(y) g_2(y)] \\ &\times \{ -8y + (Re/2) [a b f_1(y) g_1(y) \\ &+ d e f_2(y) g_2(y)] \} dy - \int_{-\frac{1}{2}}^{\frac{1}{2}} [a^2 8 y f_1(y) g_1(y) \\ &+ d^2 8 y f_2(y) g_2(y)] dy = 0. \end{aligned} \quad (33)$$

The first term on the left-hand side of equation (33) represents the energy introduced into the vortex rolls from the mean flow by means of the Reynolds stress and the second term the energy dissipated by viscosity.

The y- and z-directional energy balance equation for the first type vortex roll takes the following form:

$$\begin{aligned} &\frac{Gr}{Re^2} \int_{-\frac{1}{2}}^{\frac{1}{2}} b c g_1(y) i_1(y) dy - \tfrac{1}{2} \int_{-\frac{1}{2}}^{\frac{1}{2}} b^2 e \\ &\times \left\{ g_1(y) \left[g_1(y) \frac{dg_2(y)}{dy} + g_2(y) \frac{dg_1(y)}{dy} \right] \right. \\ &- \alpha_1 [g_1(y) \langle 2 h_1(y) g_2(y) + g_1(y) h_2(y) \rangle] \\ &+ h_1(y) \left[g_1(y) \frac{dh_2(y)}{dy} - g_2(y) \frac{dh_1(y)}{dy} \right. \\ &\left.\left. - \alpha_1 h_1(y) h_2(y) \right] \right\} dy - \frac{(Gr)_1}{Re^2} \\ &\times \int_{-\frac{1}{2}}^{\frac{1}{2}} b^2 g_1(y) i_1(y) dy = 0. \end{aligned} \quad (34)$$

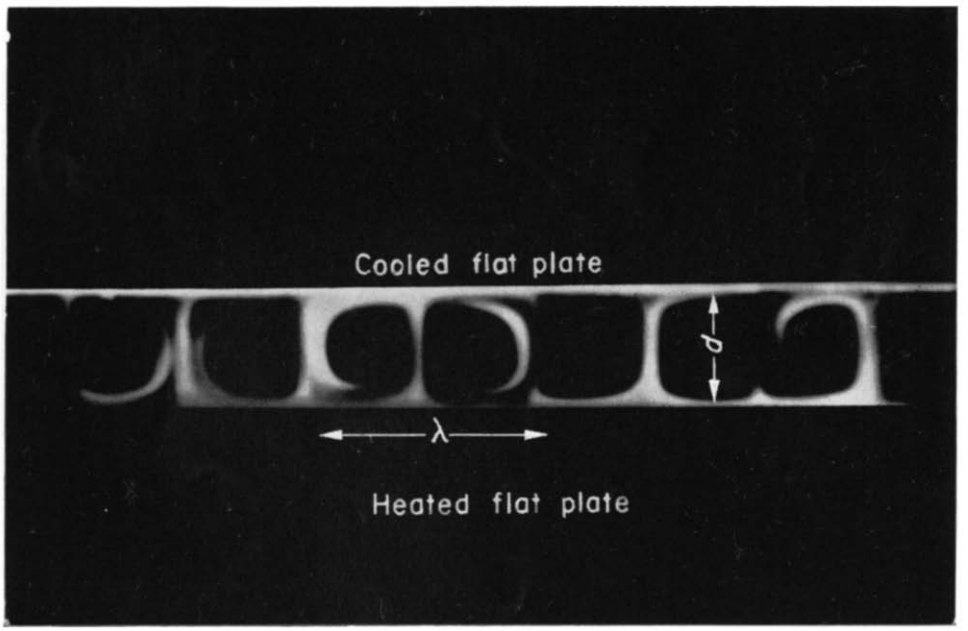

FIG. 4. Flow pattern.

[*facing page 808*

The first term on the left-hand side of equation (34) represents the energy introduced into the first type vortex roll by means of buoyancy, the second term the energy given by the first type vortex roll to the second type vortex roll and the third term the energy dissipated by viscosity. The symbol $(Gr)_1$ in equation (34) means a critical Grashof number for the first type vortex roll whose wave number is equal to 3·13. Therefore, $(Gr)_1 = (Ra)_1/Pr = 1708/Pr$.

The y- and z-directional energy balance equation for all the vortex rolls is given as follows:

$$(Gr/Re^2)\int_{-\frac{1}{2}}^{\frac{1}{2}}[b\,c\,g_1(y)\,i_1(y) + e f g_2(y)\,i_2(y)]\,dy - (1/Re^2)\int_{-\frac{1}{2}}^{\frac{1}{2}}[b^2\,(Gr)_1\,g_1(y)\,i_1(y) + e^2\,(Gr)_2\,g_2(y)\,i_2(y)]\,dy = 0. \quad (35)$$

The first term on the left-hand side of equation (35) represents the energy introduced into the vortex rolls by means of buoyancy, and the second term, the energy dissipated by viscosity. In equation (35), $(Gr)_2$ means a critical Grashof number for the second type vortex roll whose wave number is equal to 6·26 and is given as $(Gr)_2 = (Ra)_2/Pr = 18352/Pr$.

The equations of the entropy production balance are derived using energy equation (6).

Equation (31) is substituted into equation (6) and then each term is multiplied by $c\,i_1(y)\cos\alpha_1 z$ (temperature component of the first type vortex roll). Taking the average value of the above equation, we obtain the following:

$$-\left\{-\int_{-\frac{1}{2}}^{\frac{1}{2}} b\,c\,g_1(y)\,i_1(y)\,dy + \frac{Pr\,Re}{2}\int_{-\frac{1}{2}}^{\frac{1}{2}} b\,c\,g_1(y)\,i_1(y)\,[b\,c\,g_1(y)\,i_1(y) + e f g_2(y)\,i_2(y)]\,dy - \frac{Pr\,Re}{2}\int_{-\frac{1}{2}}^{\frac{1}{2}}[b\,c\,g_1(y)\,i_1(y) + e f g_2(y)\,i_2(y)]\,dy \times \int_{-\frac{1}{2}}^{\frac{1}{2}} b\,c\,g_1(y)\,i_1(y)\,dy\right\} - \left\{\tfrac{1}{2}\int_{-\frac{1}{2}}^{\frac{1}{2}} c\,i_1(y) \times \left[b f g_1(y)\frac{di_2(y)}{dy} + c e g_2(y)\frac{di_1(y)}{dy}\right]dy - \frac{\alpha_1}{2}\int_{-\frac{1}{2}}^{\frac{1}{2}} c\,i_1(y)\,[2\,b f h_1(y)\,i_2(y) + c e i_1(y)\,h_2(y)]\,dy\right\} - \int_{-\frac{1}{2}}^{\frac{1}{2}} c^2\,g_1(y)\,i_1(y)\,dy = 0. \quad (36)$$

Equation (36) indicates the entropy production balance for the first type vortex roll. The first term on the left-hand side of equation (36) represents the entropy production due to the correlation between the mean flow and the fluctuation, the second term the entropy production due to the correlation between the first and the second type vortex rolls and the third term the entropy production due to heat conduction induced by the first type vortex roll. Equation (36) shows that the first type vortex roll exists by such an entropy production balance mechanism.

Through the same calculations, the equation of the entropy production balance for all of the vortex rolls is as follows:

$$-\left\{-\int_{-\frac{1}{2}}^{\frac{1}{2}}[b\,c\,g_1(y)\,i_1(y) + e f g_2(y)\,i_2(y)]\,dy + (Pr\,Re/2)\int_{-\frac{1}{2}}^{\frac{1}{2}}[b\,c\,g_1(y)\,i_1(y) + e f g_2(y)\,i_2(y)]^2\,dy - (Pr\,Re/2) \times \left\langle \int_{-\frac{1}{2}}^{\frac{1}{2}}[b\,c\,g_1(y)\,i_1(y) + e f g_2(y)\,i_2(y)]\,dy\right\rangle^2\right\} - \int_{-\frac{1}{2}}^{\frac{1}{2}}[c^2\,g_1(y)\,i_1(y) + f^2\,g_2(y)\,i_2(y)]\,dy = 0. \quad (37)$$

The first term on the left-hand side of equation (37) represents the entropy production due to the correlation between the mean flow and the fluctuation and the second term the entropy production due to heat conduction induced by the vortex rolls.

For the six unknowns, a, b, c, d, e, f, there exist six equations, equations (32) to (37). Therefore, we can solve them.

When the Rayleigh number was increased to near $(Ra)_2$. it was observed experimentally that the vortex motion became irregular and unstable. So we study the range of Rayleigh numbers between $(Ra)_1$ and $(Ra)_2$.

By the use of the result of the eigenvalue problem of equations (20) to (22), it is shown that in the range of $Ra < (Ra)_2$ the second type vortex roll cannot exist. However, it is indicated by experimental results that in such a range of Rayleigh number the second type vortex roll pattern exists. This inconsistency can be explained as follows.

As was stated before, when a flow is fully developed, there are two different kinds of energy introduced into the vortex roll. One is the energy introduced into the vortex roll from the mean flow by means of Reynolds stress and the other is the energy introduced into the vortex roll by means of buoyancy. The eigenvalue problem controls the vortex roll components that exist in the energy due to buoyancy. Therefore, according to the result of the eigenvalue problem, the vortex roll components, whose energy is supplied by buoyancy, cannot exist in the range of $(Ra)_1 < Ra < (Ra)_2$. However, the other vortex roll components, whose energy is supplied by the Reynolds stress, can exist in such a range of Rayleigh numbers. As is clear from equations (32) to (35), the vortex roll components that derive their energy from buoyancy are the y- and z-directional components (v' and w') and the other component (u') derives its energy from the Reynolds stress.

According to the above consideration, we place the amplitude of the y- and z-directional velocity components of the second type vortex roll equal to zero. That is, we make $e = 0$. This is confirmed by Fig. 4 which indicates the flow pattern obtained by means of paraffin smoke.

As the second type vortex roll lacks the y- and z-directional velocity components, it does not exhibit a vortex pattern any more. It is more reasonable to treat the second type vortex roll as a velocity fluctuation. Then the second type vortex roll corresponds to the second harmonic of the first type vortex roll, and for this reason we assumed that the wave number of the second type vortex roll was twice that of the first type vortex roll.

To solve equations (32) to (37), the integrals contained in them are evaluated.

$$\int_{-\frac{1}{2}}^{\frac{1}{2}} 8\, y f_1(y)\, g_1(y)\, \mathrm{d}y = 1{\cdot}017 \times 10^{-2}\, Re$$

$$\int_{-\frac{1}{2}}^{\frac{1}{2}} \{f_1(y)\, g_1(y)\}^2\, \mathrm{d}y = 6{\cdot}726 \times 10^{-5}\, Re^2$$

$$\int_{-\frac{1}{2}}^{\frac{1}{2}} \{f_1(y)\, g_1(y)\, [\mathrm{d}f_2(y)/\mathrm{d}y] - 2\alpha_1 f_1(y) f_2(y)\, h_1(y)\}\, \mathrm{d}y = 1{\cdot}179 \times 10^{-3}\, Re^2$$

$$\int_{-\frac{1}{2}}^{\frac{1}{2}} 8\, y f_2(y)\, g_2(y)\, \mathrm{d}y = 2{\cdot}200 \times 10^{-2}\, Re$$

$$\int_{-\frac{1}{2}}^{\frac{1}{2}} g_1(y)\, i_1(y)\, \mathrm{d}y = 1{\cdot}764 \times 10^{-2}\, Pr\, Re$$

$$\int_{-\frac{1}{2}}^{\frac{1}{2}} \{g_1(y)\, i_1(y)\}^2\, \mathrm{d}y = 5{\cdot}285 \times 10^{-4}\, (Pr\, Re)^2$$

$$\int_{-\frac{1}{2}}^{\frac{1}{2}} \{g_1(y)\, i_1(y)\, [\mathrm{d}i_2(y)/\mathrm{d}y] - 2\alpha_1\, i_1(y)\, i_2(y) \times h_1(y)\}\, \mathrm{d}y = 1{\cdot}691 \times 10^{-4}\, (Pr\, Re)^2$$

$$\int_{-\frac{1}{2}}^{\frac{1}{2}} g_2(y)\, i_2(y)\, \mathrm{d}y = 5{\cdot}250 \times 10^{-3}\, Pr\, Re.$$

Substituting these values into each term, we solve the equations. The results are

$$a = \frac{\dfrac{64{\cdot}35}{Pr\, Re}\left\{\dfrac{Ra}{(Ra)_1} - 1\right\}^{\frac{1}{2}}}{\dfrac{3{\cdot}960}{Pr^2}\left\{\dfrac{Ra}{(Ra)_1} - 1\right\} + 5{\cdot}083} \tag{38}$$

$$b = \frac{12{\cdot}66}{Pr\, Re}\left\{\frac{Ra}{(Ra)_1} - 1\right\}^{\frac{1}{2}} \tag{39}$$

$$c = \frac{12{\cdot}66}{Pr\, Re}\left\{\frac{(Ra)_1}{Ra}\left[1 - \frac{(Ra)_1}{Ra}\right]\right\}^{\frac{1}{2}} \tag{40}$$

$$d = \frac{\frac{21{\cdot}82}{Pr^2\,Re}\left\{\frac{Ra}{(Ra)_1} - 1\right\}}{\frac{3{\cdot}960}{Pr^2}\left\{\frac{Ra}{(Ra)_1} - 1\right\} + 5{\cdot}083} \quad (41)$$

$$e = 0 \quad (42)$$

$$f = \frac{2{\cdot}580}{Pr\,Re}\left\{1 - \frac{(Ra)_1}{Ra}\right\}. \quad (43)$$

Using equations (7), (8), and (38) to (43). we get the distribution of the mean flow, as follows:

$$\bar{u} = (1 - 4y^2) + Re\int_{\frac{1}{2}}^{y} \overline{u'v'}\,dy$$

$$= (1 - 4y^2) + \frac{\frac{407{\cdot}4}{Pr^2\,Re}\left\{\frac{Ra}{(Ra)_1} - 1\right\}}{\frac{3{\cdot}960}{Pr^2}\left\{\frac{Ra}{(Ra)_1} - 1\right\} + 5{\cdot}083} \int_{\frac{1}{2}}^{y} f_1(y)\,g_1(y)\,dy \quad (44)$$

$$\bar{T} = (-y + \tfrac{1}{2} + T_u) + Pr\,Re\left\{\int_0^y \overline{v'T'}\,dy - y\int_{-\frac{1}{2}}^{\frac{1}{2}} \overline{v'T'}\,dy\right\} = (-y + \tfrac{1}{2} + T_u)$$

$$+ \frac{160{\cdot}2}{Pr\,Re}\left\{1 - \frac{(Ra)_1}{Ra}\right\}$$

$$\times \left[\tfrac{1}{2}\int_0^y g_1(y)\,i_1(y)\,dy - y\int_0^{\frac{1}{2}} g_1(y)\,i_1(y)\,dy\right]. \quad (45)$$

The second terms on the right-hand side of equations (44) and (45) show the distortion of the mean flow caused by the non-linear effect of the fluctuation components.

The results are rearranged as follows.

$$u = \bar{u} + a f_1(y)\cos\alpha_1 z + d f_2(y)\cos 2\alpha_1 z \quad (46)$$

$$v = b\,g_1(y)\cos\alpha_1 z + e\,g_2(y)\cos 2\alpha_1 z \quad (47)$$

$$w = b\,h_1(y)\sin\alpha_1 z + e\,h_2(y)\sin 2\alpha_1 z \quad (48)$$

$$T = \bar{T} + c\,i_1(y)\cos\alpha_1 z + f i_2(y)\cos 2\alpha_1 z. \quad (49)$$

In the above equations, a–f and $f_1(y)$–$i_2(y)$ are determined by equations (38) to (43) and (23) to (30), respectively. The mean flow distribution, $\bar{u}$ and $\bar{T}$, are expressed by equations (44) and (45).

The Nusselt number for this flow is

$$Nu = -\left.\frac{\partial \bar{T}}{\partial y}\right|_{y=-\frac{1}{2}} = 1 + 1{\cdot}413\left\{1 - \frac{(Ra)_1}{Ra}\right\}. \quad (50)$$

The second term on the right-hand side of equation (50) corresponds to convected heat.

3. EXPERIMENT

3.1 *Experimental apparatus*

The heated flat plate used for the experiment is shown in Fig. 5. The upper surface of the heated flat plate was made of mirror-like brass plate, and was heated by electricity. The heaters were divided into nine segments in the direction of the flow and each heater was controlled independently. In the direction normal to the flow, each heater was divided into one main heater and two compensating heaters, one on each side. The surface temperature of the flat plate was measured by copper–constantan thermocouples soldered to the brass plate. The input voltage for each heater was so regulated that the surface temperature was kept constant.

The leading edge of the heated flat plate was shaped to form an ellipse and a small pipe with a slit was buried in it. Paraffin smoke was supplied into the stream through this slit for flow visualization (see Fig. 4).

The cooled flat plate, which was made of transparent vinyl plates, was mounted on the heated flat plate. Its surface temperature was kept constant by means of cooling water. The height of the flow passage was adjusted by the height of side walls.

To avoid disturbance caused by the measuring slits, a flat plate was laid above the cooled flat plate. The distance from this flat plate to the cooled flat plate was equal to the height of the flow passage.

Even if the flow has a high velocity, it becomes three-dimensional so long as the temperature difference is large enough to cause the vortex rolls. For instance, if the temperature

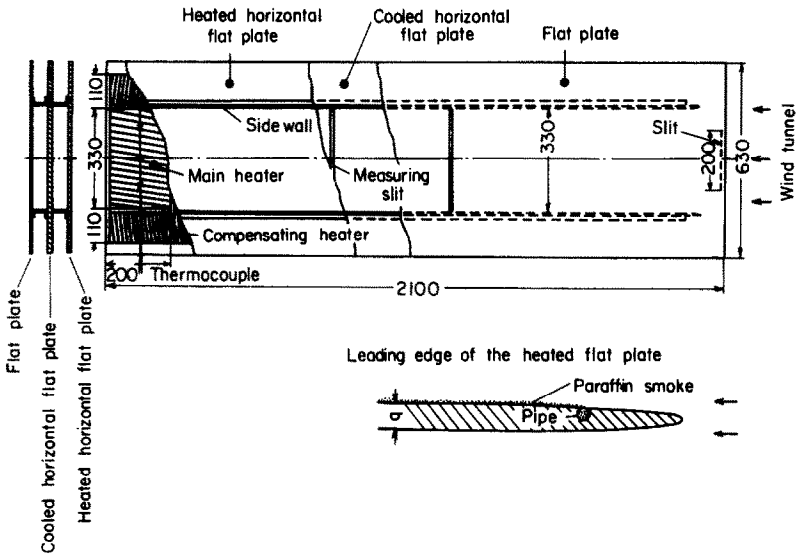

FIG. 5. Experimental apparatus.

difference is about 60 degC, a flow field along the heated flat plate, whose main stream velocity is about 3 m/s, becomes three-dimensional near the rear part of the heated flat plate. However, we used a low speed flow ($U_0 \doteqdot 0{\cdot}6$ m/s) in this experiment to get a stable fully developed flow.

Because of the low speed and because of the existence of the temperature field, the special hot-wire anemometer which is shown in Fig. 6 was used to measure flow velocity. The transmitter shown in Fig. 6 consists of a platinum wire of 50 μ diameter which is stretched normal to the flow direction and an A.C. current at 50 cycles is supplied to it. The receiver is a fine platinum wire of 5 μ diameter and is heated by a constant current. The transmitter is fixed, but the receiver can be traversed in the flow direction so as to adjust the distance between them.

A heat signal of 100 cycles is added to the flow which passes the transmitter and this signal is transported to the receiver by the flow. The signal is received as a voltage fluctuation in the receiver. Denoting the voltage applied to the transmitter by $e_1 \propto \sin \omega t$, the signal voltage e_2 detected by the receiver is proportional to $\sin^2[\omega t - (2\pi/T)(l/u)]$, where u is the velocity of the flow, l is the distance from the transmitter to the receiver, $T = 1/50$ and $\omega = 100\,\pi$. If we change the distance, the received signal changes from e_2 to e_2', where e_2' is proportional to

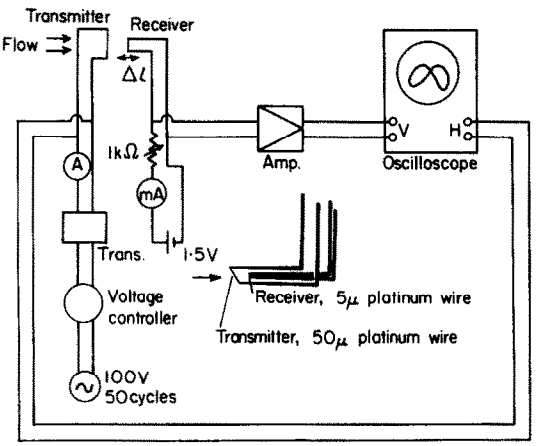

FIG. 6. Hot-wire anemometer.

$\sin^2\{\omega t - [(2\pi/T)(l/u) + (2\pi/T)(\Delta l/u)]\}$. Applying e_1 and $e_2(e_2')$ to the horizontal and the vertical deflectors of the oscilloscope, respectively, we observe a Lissajous figure on the screen.

If we select l and Δl as $[(2\pi/T)(l/u) = (\pi/2)\,m]$ (m is a positive integer) and $[(2\pi/T)(\Delta l/u) = (\pi/2)]$, the Lissajous figure for each case becomes a parabola whose convex direction is reversed. The velocity of the flow is measured by the observation of these parabolas. After putting the receiver at the place which makes a parabola appear on the screen of the oscilloscope, we shift it to the new place which again makes a parabola appear on the screen. If we can measure the shifted distance Δl, the velocity of the flow is known, using the relation $[(2\pi/T)(\Delta l/u) = (\pi/2)]$, as $u = 200\,\Delta l$ (1/s).

An increase in m weakens the received signal, so we used the state of $m = 1$. In such a state, the receiver was slightly affected by the wake of the transmitter. The correction for this wake was made.

The temperature of the fluid measured by a copper–constantan thermocouple, made of 0·1 mm wires, and a potentiometer. Lead wires of the thermocouple were contained in a stainless-steel tube of 0·8 mm outer diameter and only the tip of the thermocouple was exposed. In order to eliminate the effect of the measuring slit and to prevent errors due to heat conduction, the stainless-steel tube was bent to an L-shape.

3.2 *Experimental results*

3.2.1 *The velocity distribution.* Measurements were made to confirm whether a velocity distribution was fully developed or not when there was no temperature difference, and the result is shown in Fig. 7. It is clear from Fig. 7 that the velocity distribution is fully developed at the measuring station ($x = 1550$ mm) and there is no effect attributable to the paraffin smoke.

Experimental results for the flow with vortex rolls are shown in Figs. 8 and 9. Figures 8 and 9 indicate the velocity distribution in the y- and z-direction, respectively. The heavy lines in these figures are analytical values due to equation (46). Experimental results are in good agreement with analytical results. Figure 9(b) indicates the velocity distribution in the middle plane of the passage. If there existed only the

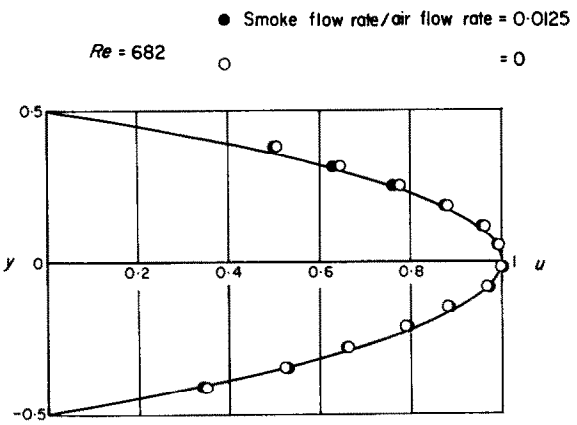

FIG. 7. Fully developed velocity distribution.

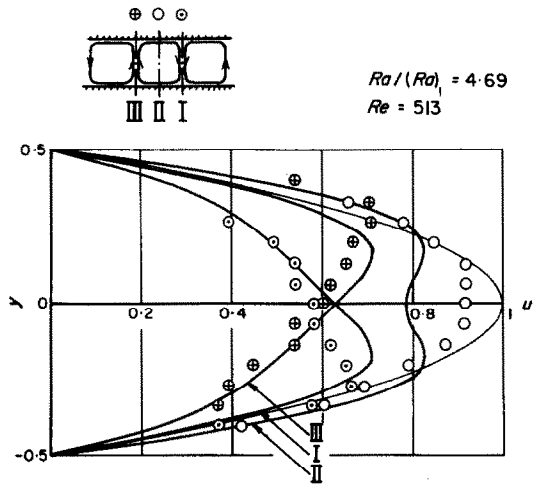

FIG. 8. Velocity distribution.

first type vortex rolls, this velocity distribution would indicate a constant value. Because of the existence of the second type velocity fluctuation whose pitch is a half of the first type vortex roll, the velocity distribution is distorted as is shown in Fig. 9.

3.2.2 *The temperature distribution.* Figure 10 indicates the temperature distribution of a flow with no vortex roll. It is shown by this figure that the temperature distribution is not fully developed in the range of experimental Reynolds numbers. But, as is indicated in Fig. 11, the appearance of the vortex rolls accelerates the development of the temperature distribution.

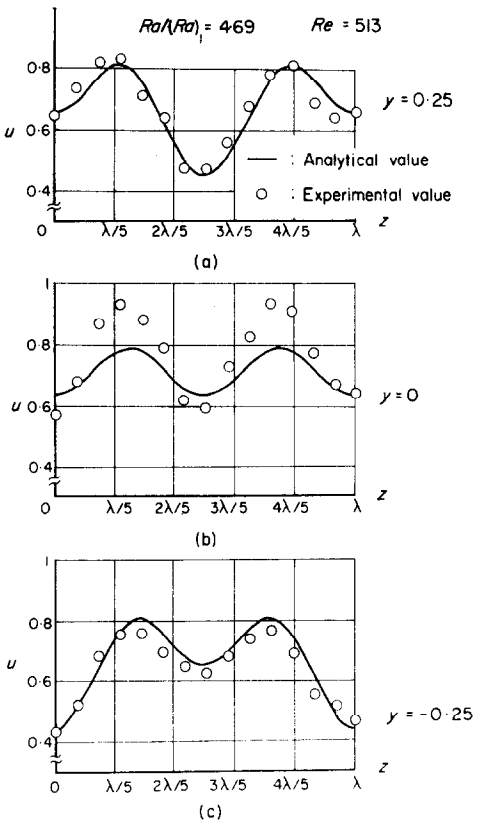

FIG. 9. Velocity distribution.

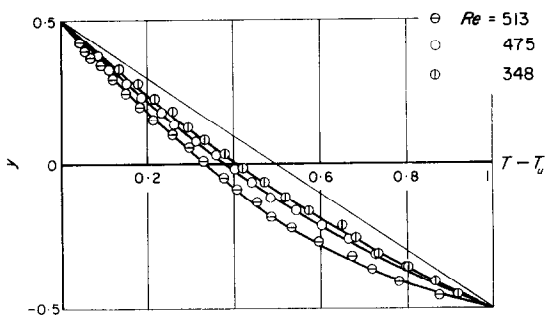

FIG. 10. Temperature distribution ($Ra < (Ra)_1$).

Experimental results for a flow with vortex rolls are shown in Figs. 12 and 13. Figures 12 and 13 indicate the temperature distribution in the y- and z-direction, respectively. The heavy lines in the figures are analytical values due to equation (49). The line of dashes in Fig. 12 indicates the distribution of $\bar{T}(y)$ due to equation (45), and it is found from this figure that the temperature gradient $\partial\bar{T}/\partial y$ reverses itself in the middle part of the passage. It is seen from this fact that heat is conducted from the upper cooled flat plate to the lower heated flat plate in such a region. As the heat flow from the lower to the upper flat plate is constant, there must be a violent convection motion in the middle of the passage to compensate for the negative heat conduction. The distribution of $\bar{T}(y)$ cannot be measured experimentally, but in the range of experimental Rayleigh numbers it is possible to approximate the $\bar{T}(y)$ distribution by the central distribution of the vortex roll (shown by the line connecting open circles). This distribution does not indicate the reversal of the temperature gradient, but in the middle of the passage the temperature gradient decreases to near zero. Therefore, it was found experimentally that the heat is transferred by convection in the middle part of the passage. As is shown in Fig. 12, there is a little difference between the experimental and the analytical values. This might be caused by the error of the approximate analytical method. Figure 13 shows the temperature distribution in the z-direction. It is found from this figure that the temperature distribution is distorted away from the sinusoidal distribution by the effect of the second type fluctuation.

3.2.3 *The pitch of vortex rolls.* The variation of λ due to the change of d, Re and Ra is investigated experimentally and the result is shown in Fig. 14. Figure 14 indicates that, in the range of $d < 15$ mm, λ depends only on the value of d, and, in the range of $d > 15$ mm, λ remains constant, unaffected by Re, Ra and d. The relation between d and λ in the range of $d < 15$ mm is expressed as $\lambda = 2{\cdot}0\,d$. This relation agrees with the one that was predicted by the linearized theory.

In the case of a flow along a heated horizontal flat plate, that is, in the case of the height d of the passage equal to infinity, it is inferred from

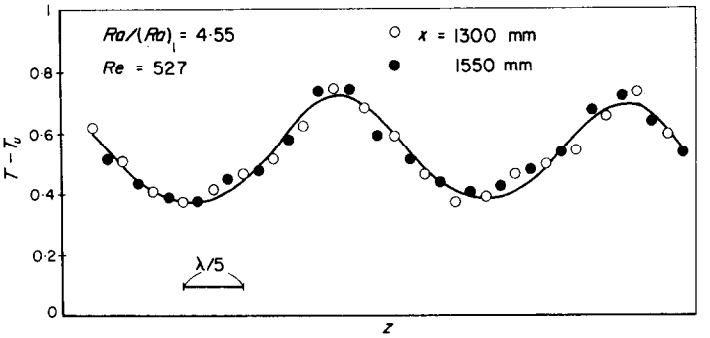

FIG. 11. Temperature distribution.

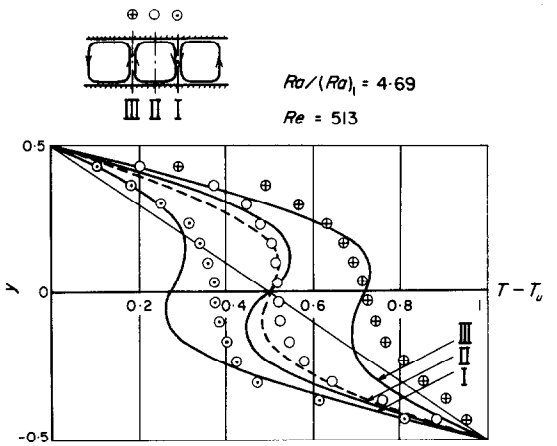

FIG. 12. Temperature distribution.

this experimental result that the vortex roll whose pitch is 32·2 mm appears. Therefore, the well-known result [5, 6] about two-dimensional heat transfer from a heated horizontal flat plate can only be used when the temperature difference is small and no vortex rolls appear on the flat plate.

3.2.4 *Nusselt number.* The increase of the Nusselt number due to the appearance of vortex rolls was calculated from the experimental results and is shown in Fig. 15. The heavy line in Fig. 15 is the analytical value due to equation (50). To determine the experimental Nusselt number, the temperature gradient at the surface of the heated flat plate was used. In the range of $Ra < (Ra)_1$ there exists no vortex roll in the passage and the flow is two-dimensional. But in the range of $Ra > (Ra)_1$ the vortex rolls appear and the flow becomes three-dimensional. Heat due to convection rapidly increases with Rayleigh number and the Nusselt number becomes larger than 1.

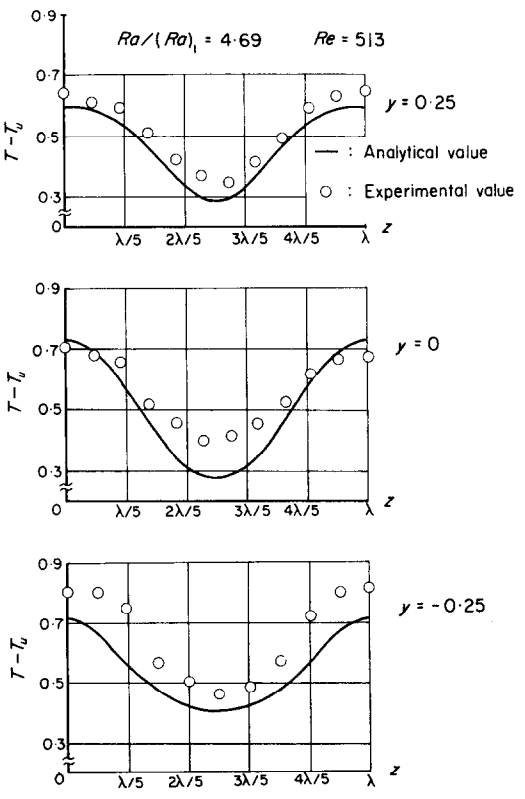

FIG. 13. Temperature distribution.

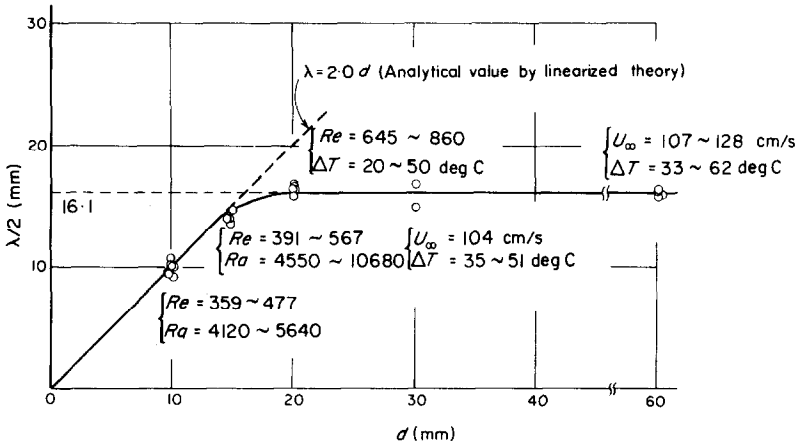

FIG. 14. Pitch of vortex rolls.

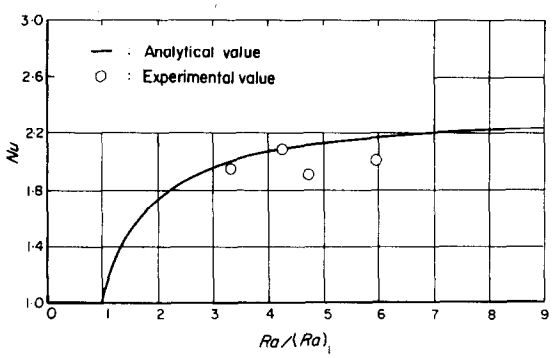

FIG. 15. The Nusselt number.

4. CONCLUSION

By investigating the forced convective heat transfer between horizontal flat plates, when the lower plate is heated and the upper is cooled under the condition of a steady fully developed flow, we obtained the following conclusions.

(a) A sufficiently large temperature difference between the flat plates causes a three-dimensional flow. It was clarified by the experiment and analysis that this three-dimensional character was caused by vortex rolls whose axes were parallel to the flow direction.

(b) The Navier–Stokes equations and the energy equation for a three-dimensional flow were solved by an approximate method taking into account the nonlinear effect of the fluctuations. In the process of solving these equations, the mechanism of the vortex rolls was clarified and it was found that these discrete vortex rolls could be a simple model of turbulent flow.

(c) The Nusselt number for a three-dimensional flow was obtained analytically. It was shown that the Nusselt number rapidly increased with the appearance of the vortex rolls.

(d) A quantitative experiment on the vortex rolls was made. Experimental results for the velocity distribution, the temperature distribution, the pitch of the vortex rolls and the Nusselt number were obtained. These experimental results were compared with analytical results, and it was found that they were in good agreement.

REFERENCES

1. W. V. R. MALKUS, Discrete transition in turbulent convection, *Proc. R. Soc.* **A225**, 185–195 (1954); The heat transport and spectrum of thermal turbulence, *Proc. R. Soc.* **A225**, 196–212 (1954).
2. W. V. R. MALKUS and G. VERONIS, Finite amplitude cellular convection, *J. Fluid Mech.* **4**, 225–260 (1958).
3. J. T. STUART, On the non-linear mechanics of hydrodynamic stability, *J. Fluid Mech.* **4**, 1–21 (1958).
4. A. PELLEW and R. V. SOUTHWELL, On maintained convection motion in a fluid heated from below, *Proc. R. Soc.* **A176**, 312–343 (1940).
5. YASUO MORI, Buoyancy effects in forced laminar convection flow over a horizontal flat plate, *J. Heat Transfer* **83**, 479–482 (1961).
6. E. M. SPARROW and J. MINKOWYCZ, Buoyancy effects on horizontal boundary-layer flow and heat transfer, *Int. J. Heat Mass Transfer* **5**, 505–511 (1962).

Résumé—On peut considérer comme bidimensionnel l'écoulement entièrement établi et le champ de température entre deux plaques planes horizontales (lorsque la plaque inférieure est chauffée et la plaque supérieure est refroidie). Cependant, lorsque la différence de température entre ces plaques planes dépasse un valeur critique, on observe l'apparition de tourbillons en rouleaux dont les axes sont parallèles à la direction de l'écoulement. En conséquence, les champs de vitesse et de température sont complètement modifiés par ces tourbillons en rouleaux et ont un caractère tridimensionnel. Les équations de la quantité de mouvement et de l'énergie pour de tels champs sont non-linéaires. Ces équations sont résolues approximativement en se basant sur les bilans d'énergie et de production d'entropie des tourbillons en rouleaux. Afin d'obtenir des résultats théoriques, on a mesuré les distributions de vitesse et de température de l'écoulement tridimensionnel. On trouve que les résultats théoriques sont en bon accord avec les résultats expérimentaux.

Zusammenfassung—Für voll ausgebildete Strömungen und Temperaturfelder zwischen zwei ebenen waagerechten Platten (wobei die untere Platte beheizt und die obere gekühlt ist), können zweidimensionale Verteilungen angenommen werden. Wird jedoch die Temperaturdifferenz zwischen diesen Platten über einen kritischen Wert gesteigert, so erscheinen zwischen den ebenen Platten Wirbelrollen, deren Achsen parallel zur Strömungsrichtung liegen. Somit werden die Strömungs- und Temperaturfelder von diesen Wirbelrollen beeinflusst und nehmen einen dreidimensionalen Charakter an. Die Bewegungs- und Energiegleichungen dieser Felder sind nichtlinear. Diese Gleichungen sind auf Grund der Energie- und Entropiebilanz näherungsweise gelöst. Um theoretische Ergenisse zu erhalten, wurden die Geschwindigkeits- und Temperaturverteilungen der dreidimensionalen Strömung ausgemessen. Die theoretischen Ergebnisse zeigten gute Übereinstimmung mit den experimentallen.

Аннотация—При полностью развитых течениях и наличии температурных полей между горизонтальными плоскими пластинами (когда нижняя пластина нагрета, а верхняя охлаждена) процесс теплопереноса можно было бы считать двумерным. Однако при увеличении разности температур между этими пластинами выше критического значения возникают вращения, ось которых параллельна направлению течения. Под влиянием этих вихревых вращений температурное поле получает трехмерный характер. Уравнения количества движения и энергии для подобных полей являются нелинейными. Такие уравнения решаются приближенно на основе баланса энергии и возрастания энтропии вихревых вращении. Для подтверждения теоретических результатов измеряется распределение скорости и температуры трехмерного потока. Найдено, что теоретические результаты хорошо согласуются с экспериментальными.